Stellar Spectra A. Basic Line Formation

Andreas Ellewsen[1]

[1] Institute of theoretical astrophysics

Abstract. We learned how to write nice reports ...

1. Introduction

This is the first of three numerical exercises in the course on Radiative processes in astrophysics (AST4310) at the University of Oslo. In this exercise we are to follow the steps of Annie Cannon, Cecilia Payne, and Marcel Minnaert. By doing this we hope to learn about the use of spectral lines in astophysics.

2. Spectral Classification

The first part of this section deals with learning a little about how IDL functions. You also make a fuction that adds all the numbers in an array together and gives you the result. This function already exists in IDL, and is called TOTAL, but we make our own function anyway. The function is called ADDUP, and looks exactly like the function written in the exercise text. The function has been tested, and it passes all the test I've tried throwing at it (except of course those it will clearly fail, like strings).

The second part of this section deals with LaTeX and gives instructions on how to write a good report. Basically one is given a template and told a long list of things that are useful to know when writing reports, and then you use this knowledge for the rest of the exercise.

3. Saha-Boltzmann calibration of the Harvard sequence

Here we want to explain the spectral-type sequence that was studied in the two first parts of the last section (which we ignored). To start of we study figures 5 and 7 in the exercise text. Starting from the right of figure 5 one sees that the $H\beta$ line lies between 4762Å and 4954Å. If one looks at figure 7 one sees that the only line between these two wavelengths is the Balmer β line at 4861Å. The Balmer β line is the transition between $n = 4$ and $n = 2$. Considering that the spectrum we're looking at in figure 5 ranges between 3900Å and 5000Å, which is in the visual part of the spectrum, the rest of the lines corresponding to hydrogen should all be in the Balmer series as well. This means that none of the lines share the same upper level, and that they all share the same lower level, namely $n = 2$. This is the case for all of these named series. Sharing of the upper levels is a bit more complicated. If one looks at figure 7 one sees that Lyman α shares no upper level with anything. But Lyman β shares the same upper level as Balmer α. Figure 7 skips some of the transitions. But Lyman γ shares upper level with Balmer β and Paschen α. It keeps going in this way for the rest of the transitions.

At this point Payne made the assumption that the strength of the absorption lines observed in stellar spectra scaled with the population density of the lower level of the corresponding transition. This seems logical if one also assumes that most of the hydrogen was in the ground state to begin with.

It turns out that this assumption assumption is not correct, but in general it is true that stellar absorption lines get stronger at larger lower-level population.

We ignore this and continue with Payne's assumption anyway.

- Use this expectation to give initial rough estimates of the strength ratios of the α lines in the the H I Lyman, Balmer, Paschen and Brackett series.

The Boltzmann distribution is defined

$$\frac{n_{r,s}}{N_r} = \frac{g_{r,s}}{U_r} e^{-\chi_{r,s}/kT} \tag{1}$$

The partition function U_r is define as

$$U_r = \sum_s g_{r,s} e^{-\chi_{r,s}/kT} \tag{2}$$

The Saha law reads

$$\frac{N_{r+1}}{N_r} = \frac{1}{N_e} \frac{2U_{r+1}}{U_r} \left(\frac{2\pi m_e kT}{h^2} \right)^{3/2} e^{-}\chi_r/kT. \tag{3}$$

- Note in the first table that the partition functions computed from (2) are of order unity and barely sensitive to temperature.
- In the second table, note the steep Boltzmann population decay with $\chi_{r,s}$ given by (1). It is less steep for higher temperature. The columns add up to unit y because the values in this table are scaled by N_r. They therefore depend on U_r, but the small variation between U_1 and U_4 in the first table produces a difference at two-digit significance only for $s = 1$ at $20000K$. The partition function U_1 of the neutral stage is the sum of only seven levels; the higher levels present in stages $r \geq 2$ contribute only marginally. The ground state always has the largest population.
- Inspect the third table, computed from (3). There are only two ionization stages significantly present per column. For T = 5000 K element E is predominantly neutral, for T = 10 000 K it is once ionized (E^+), for higher temperature stages E^{2+} and E^{3+} appear while E and E^+ vanish.
- Explain from (1) and (3) why the Saha and Boltzmann distributions behave differently for increasing temperature.
- Speculate why ionization can fully deplete a stage even though excitation puts only a few atoms in levels below the ionization level. Hint: what parameter in the Saha distribution can cause equality between high-level and next-ion population at a given temperature?

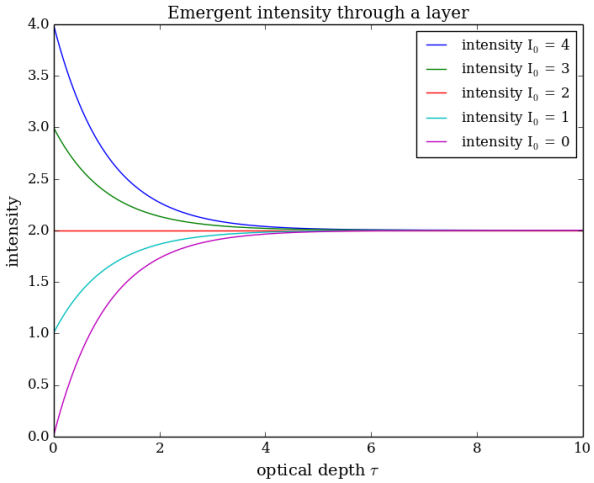

Fig. 1. As the optical depth increases, the intensity converges to the intensity of the Source function B.

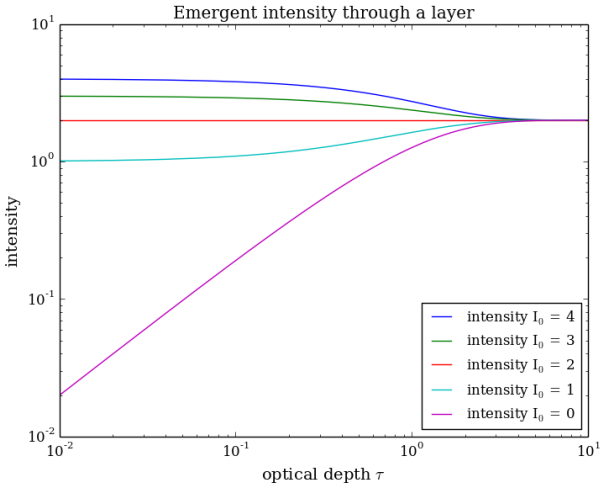

Fig. 2. The emergent intensity with a logarithimic scale.

3.1. Saha-Boltzmann population of Shadeenium

Now it is time to reproduce Shadee's tables. This is done by using python routines to compute U_r from (2) and $n_{r,s}/N_r$ from (1), and N_r/N from (3) for element E. All computations are done using cgs units.

4. Fraunhofer line strengths and the curve of growth

4.1. Radiation through an isothermal layer

It can be shown that the total emergent radiation from a layer with optical thickness $\tau(x)$ and temperature $T(x)$ is:

$$I_\lambda = I_\lambda(0)e^{-\tau} + \int_0^\tau B_\lambda[T(x)]e^{-(\tau-\tau(x))}d\tau(x) \tag{4}$$

If one assumes that the layer is isothermal, this implies that the optical thickness and temperature is independent of position inside the layer. Inserting this into equation 4 gives the following

$$\begin{aligned} I_\lambda =& I_\lambda(0)e^{-\tau} + \int_0^\tau B_\lambda[T(x)]e^{-(\tau-\tau(x)')}d\tau(x)' \\ =& I_\lambda(0)e^{-\tau} + B_\lambda(T)e^{-\tau}\int_0^\tau e^{\tau'}d\tau' \\ =& I_\lambda(0)e^{-\tau} + B_\lambda(T)e^{-\tau}(e^\tau - 1) \end{aligned}$$

$$I_\lambda = I_\lambda(0)e^{-\tau} + B_\lambda(1 - e^{-\tau}) \tag{5}$$

Studying figures 1 & 2 shows a few different things. If one first considers cases where $\tau << 1$, the figures show that if $I_\lambda(0) = 0$, you get an exponential growth due to the source function B. And if $I_\lambda(0) > B_\lambda$ the intensity stays close to constant. This case corresponds to an "optically thin" medium. This is because whatever intensity that enters the medium passes straight through without being affected by the medium.

The opposite case where $\tau >> 1$ is called an "optically" thick medium, since all the incident radiation is absorbed before it is able to pass through, and is replaced by the radiation emitted by the medium itself. As seen in the plot, the emergent intensity becomes independent of optical depth for large τ. Mathematically this can be seen by looking at equation 5 and letting $\tau \to \infty$. In physical terms one can picture it such that both the incident radiation and the radiation emitted by the medium is absorbed while it is passing through the medium, but since the medium replenishes the radiation it is emitting along the path through it, this radiation is refilled as one goes through the medium.

From this it should be clear that optically thin mediums allow us to view radiation originating from the other side of the medium, while optically thick mediums absorb all of the incident radiation before it can pass through, thus blocking our view past them.

4.2. Spectral lines from a solar reversing layer

At this point we choose to use the Schuster-Schwarzschild model. Another name for this model is a reversing-layer model. This model works on the assumption that the continous radiation, without spectral lines, is emitted by the surface of the star, and this radiation then irradiates a seperate layer around the star. This layer is then hit by an intensity

$$I_\lambda(0) = B_\lambda(T_{surface}). \tag{6}$$

This causes emission only at the wavelengths of spectral lines. Next, ones assumes that the star is optically thick, so that the surfrace radiates with the solution of equation 5 where $\tau << 1$, meaning $I_\lambda = B_\lambda(T_{surface})$. This does not mean that shell has to be optically thick. The line-causing atoms in the shell have their own temperature T_{layer}, giving a local production of radiation in the layer for the line-wavelength $B_\lambda(T_{layer})\Delta\tau(x)$. Combining equation 5 & 4.2 yields

$$I_\lambda = B_\lambda(T_{surface})e^{-\tau_\lambda} + B_\lambda(T_{layer})(1 - e^{-\tau_\lambda}) \tag{7}$$

Note that the opaqueness τ in equation 4.2 has gotten an index for wavelength, since it depends on wavelength.

4.3. Voigt profile

In reality spectral lines are not infinitely sharp delta functions. This can be attributed to Doppler shifts and Coloumb interactions between neighbouring particles. (Even if one could get rid of those effects, you would still have the uncertainty principle spreading it out a little.)

This broadening of the spectral line is described by the distribution

$$\tau(u) = \tau(0)V(a,u) \tag{8}$$

where V is the Voigt function, and u describes the the wavelength separation from the center of the line such that

$$u \equiv \Delta\lambda/\Delta\lambda_D \tag{9}$$

where

$$\Delta\lambda_D \equiv \frac{\lambda}{c}\sqrt{2kT/m}. \tag{10}$$

Here m is the mass of the line-causing particles. The a parameter measures the the Coloumb disturbances. For stellar atomspheres a is usually somewhere in the range $0.01 - 0.5$. The definition of the Voigt function is

$$V(a,u) = \frac{1}{\Delta\lambda_D\sqrt{\pi}}\frac{a}{\pi}\int_{-\infty}^{+\infty}\frac{e^{-y^2}}{(u-y)^2+a^2}dy \tag{11}$$

The Voigt profile represents the convolution(smearing) of a Gauss profile using a Lorentz profile. Because of this it has a Gaussian shape close to line center, and Lorentzian wings on the edges. This can be approximated by taking the sum instead of the convolution giving

$$V(a,u) = \frac{1}{\Delta\lambda_D\sqrt{\pi}}\left[e^{-u^2} + \frac{a}{\sqrt{\pi}u^2}\right] \tag{12}$$

For those using IDL to do calculations, the voigt function is ready for use through the appropriately named function voigt. Since I use python we instead have to use the fact that the voigt function can be written

$$V(x;\sigma,\gamma) = \frac{Re[w(z)]}{\sigma\sqrt{2\pi}} \tag{13}$$

where Re[w(z)] is the real part of the Faddeeva function evaluated for

$$z = \frac{x+i\gamma}{\sqrt{2}\sigma}\ ,\ a = \frac{\sigma}{\sqrt{2}\sigma}\ ,\ u = \frac{x}{\sqrt{2}\sigma}.$$

In this case the factor $\Delta\lambda_D = \sqrt{2}\sigma$. Luckily for us the Faddeeva function can be found in the special module of the scipy package for python, so that is what we will be using. If we plot this function for different values of a for $u = [-10, 10]$ we get figure 3. To study this we plot the same, but this time with a logarthimic scale for the y axis. The plot can be seen in figure 4. Using approximation 4.3 it is clear that the the exponential term vanishes very quickly as $|u|$ increases, leaving us with

$$V(a,u) \approx \frac{a}{\Delta\lambda_D\pi u^2}$$

which gives the functions the same form on the wings just scaled by the factor a.

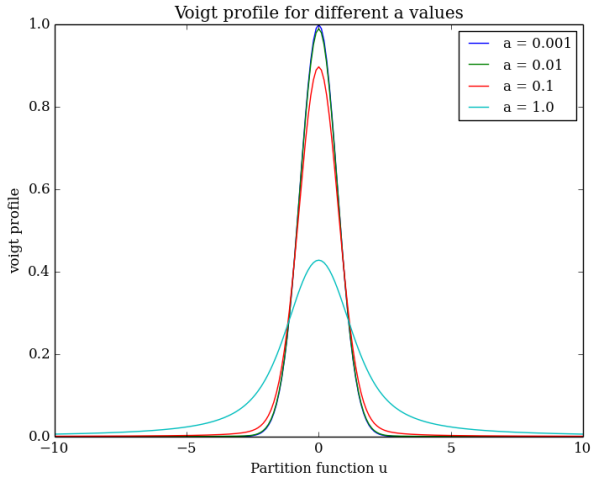

Fig. 3. Voigt profile for different values of a.

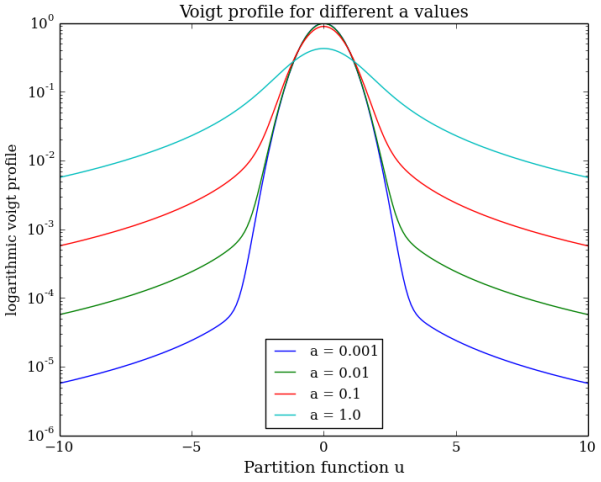

Fig. 4. Logarithmic voigt profile for different values of a.

4.4. Emergent line profiles

We now have both functions for intensity and for the distribution of the optical depth. If we now combine equation 5 & 4.3 we should be able to compute and plot stellar spectral line profiles! To do this we use values that fit well with the solar photosphere and plot what it looks like in the visible spectrum. The values we will be using are $T_{surface} = 5700K$, $T_{layer} = 4200K$, $a = 0.01$, $\lambda = 5000$Å. We start by plotting the intensity against u for $\tau(0) = 1$. This results in figure 5.

- Explain profile shapes for $\tau(0) << 1$.
- Why is there a low-intensity saturation limit for $\tau >> 1$?
- Why do the line wings develop only for very large $\tau(0)$?
- Where do the wings end?
- For which values of $\tau(0)$ is the layer optically thin,respectively optically thick, at line center? And at $u = 5$?
- Now study the dependence of these line profiles on wavelength by repeating the above for $\lambda = 2000$Å (ultraviolet) and $\lambda = 10000$Å (near infrared). What sets the top value I_{cont} and the limit value reached at line center by $I(0)$? Check these values by computing them directly on the command line. What happens to these values at other wavelengths?

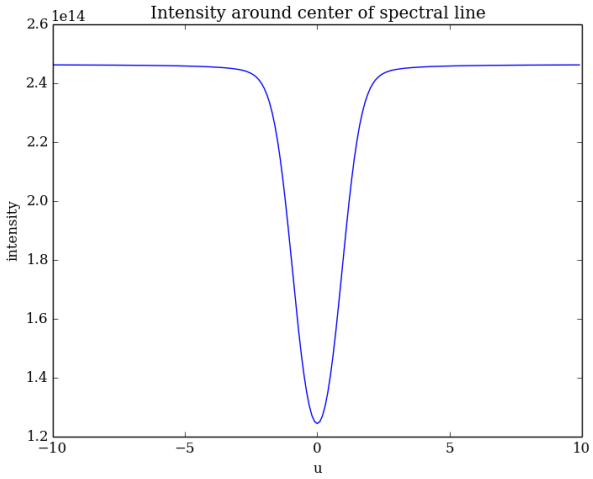

Fig. 5. Spectral lines for wavelength 5000 Å.

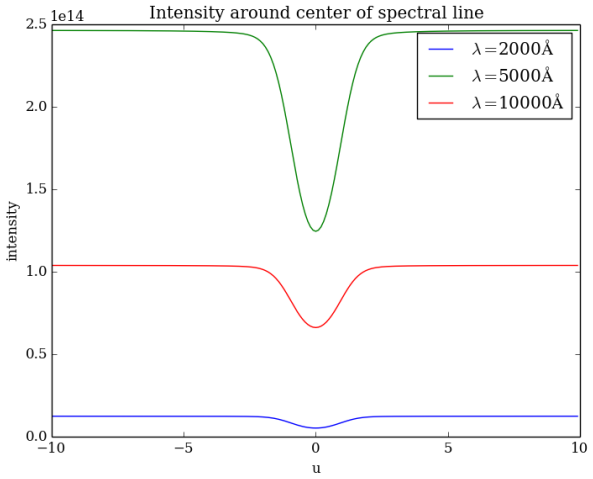

Fig. 7. Spectral lines for different wavelengths.

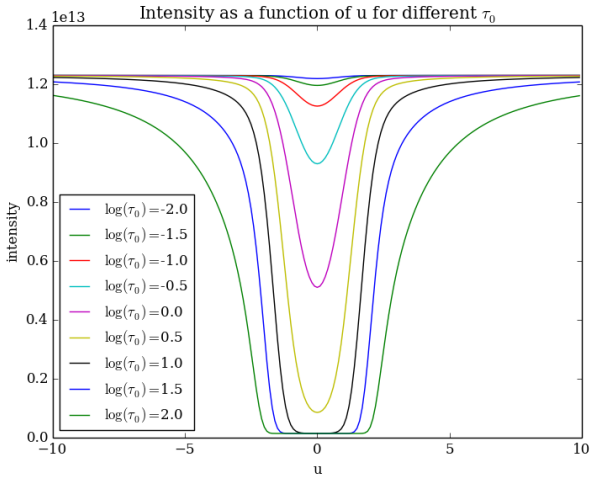

Fig. 6. Spectral lines for different choices of $\tau(0)$.

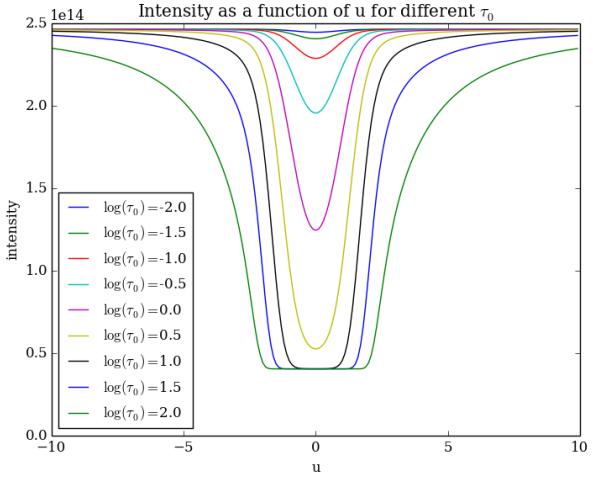

Fig. 8. Spectral lines for different choices of $\tau(0)$.

Next we study the behaviour of the line for $\tau(0)$ in the range $\log \tau(0) = [-2, 2]$. This results in figure 6. Looking at the spectral lines for different wavelengths reveal a difference in intensity. This can be seen in figure 7.

To check the behaviour for different wavelengths we plot the results for $\lambda = 5000$ & 10000 in figures 8 & 9.

- Explain profile shapes for $\tau(0) << 1$.
- Why is there a low-intensity saturation limit for $\tau >> 1$?
- Why do the line wings develop only for very large $\tau(0)$?
- Where do the wings end?
- For which values of $\tau(0)$ is the layer optically thin,respectively optically thick, at line center? And at $u = 5$?
- Now study the dependence of these line profiles on wavelength by repeating the above for $\lambda = 2000$Å (ultraviolet) and $\lambda = 10000$Å (near infrared). What sets the top value I_{cont} and the limit value reached at line center by $I(0)$? Chek these values by computing them directly on the command line. What happens to these values at other wavelengths?

Since some observed spectra are measured without absolute intensity calibration it useful to scale the spectrum to the local continuum intensity by plotting I_λ / I_{cont}. Plotting this for the same 3 wavelengths reults in figure 10.

4.5. The equivalent width of spectral lines

From the profile plots one can see that the growth of the absorption feature for increasing $\tau(0)$is faster for small $\tau(0)$ than for larger $\tau(0)$. Because of this, Minnaert and his coworkers introduced the equivalent width W_λ as a line-strength parameter to measure this effect. It measures the integrated line depression in the normalized spectrum

$$W_\lambda = \int \frac{I_{cont} - I(\lambda)}{I_{cont}} d\lambda. \tag{14}$$

To test this effectively we make a profile function that returns a Schuster-Schwarzschild profile, given a, τ, and u. Setting $a = 0.1$, $\tau(0) = 100$ and plotting this for $u = [-200, 200]$ returns figure 11

Next we compute the line depth in relative units(the integrand in equation 4.5. Plotting this versus u gives figure 12

5. Conclusions

insert conclusions

Acknowledgements.

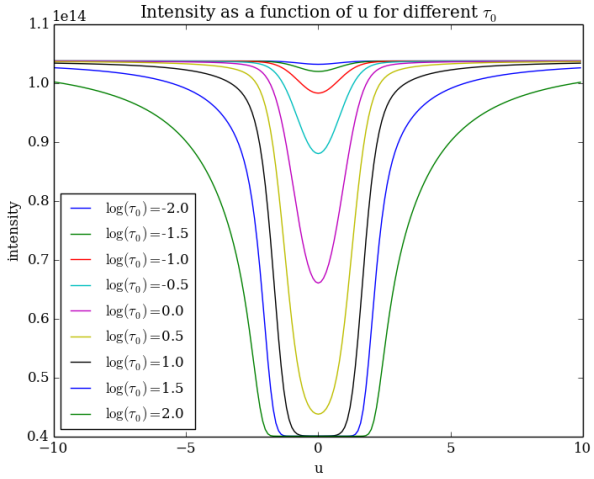

Fig. 9. Spectral lines for different choices of $\tau(0)$.

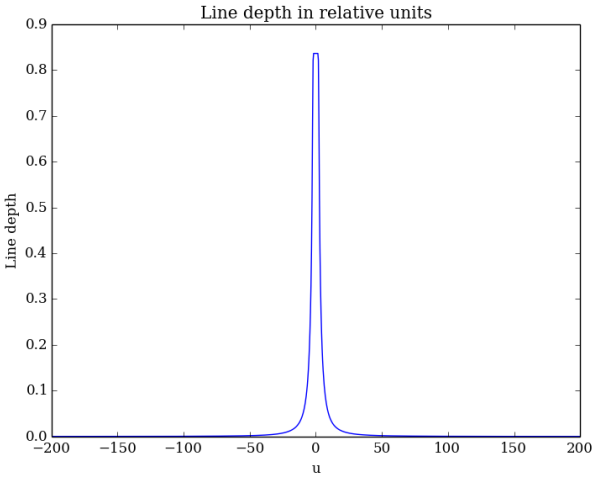

Fig. 12. Line depth in relative units.

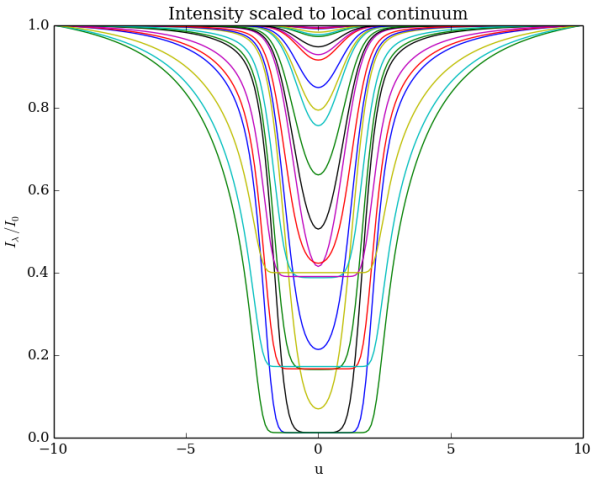

Fig. 10. Spectral lines for different choices of $\tau(0)$.

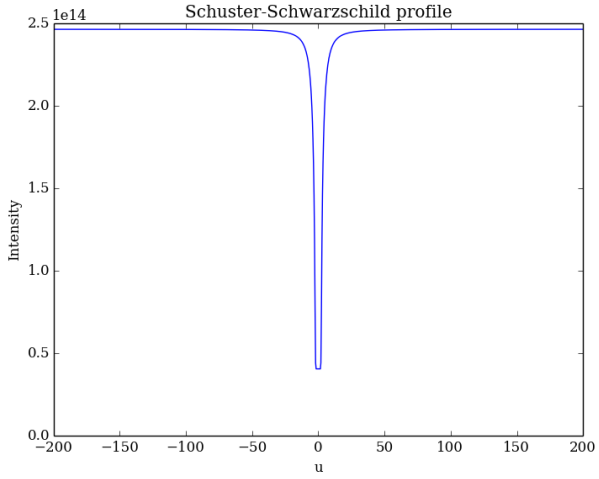

Fig. 11. Schuster-Schwarzschild profile.